Biochimica et Biophysica Acta, 1152 (1993) 69–77

BBAMEM 76086

Squalene promotes the formation of non-bilayer structures in phospholipid model membranes

Karl Lohner [a,*], Gabor Degovics [a], Peter Laggner [a], Eva Gnamusch [b] and Fritz Paltauf [b]

[a] *Institut für Biophysik und Röntgenstrukturforschung, Austrian Academy of Sciences, Steyrergasse 17/VI, A-8010 Graz (Austria) and* [b] *Institut für Biochemie und Lebensmittelchemie, Technische Universität Graz, Petersgasse 12, A-8010 Graz (Austria)*

(Received 25 May 1993)

Key words: Phosphatidylethanolamine; Hydrophobic molecule; Lipid polymorphism; DSC; X-ray diffraction

A study of the lipid polymorphism of aqueous dispersions of stearoyloleoylphosphatidylethanolamine and palmitoyloleoylphosphatidylcholine (95:5, mol/mol) in the presence of the hydrophobic molecule squalene, an intermediate in the biosynthesis of sterols, has been performed. With increasing concentration of squalene the main transition temperature was decreased from 29.8°C for the pure phospholipid system to 28.1°C for samples containing 5 mol% squalene without considerable changes in the phase transition enthalpy as detected by high precision differential scanning calorimetry. The structure of the phospholipid aggregates was determined by small- and wide-angle X-ray diffraction experiments showing only a minor increase of the lamellar repeat distance of the liquid-crystalline phase for the squalene containing samples. By far more pronounced was the effect of squalene on the lamellar-to-inverse-hexagonal phase transition, which was shifted from 64°C to about 36°C in the presence of 6 mol% squalene, thereby overlapping with the main transition. X-ray data showed that the size of the tubes of the inverse hexagonal phase are increasing linearly up to 6 mol% squalene. Experiments performed in the presence of 10 mol% squalene did not further change the phase behaviour, indicating the limiting partition of this hydrophobic molecule into the membrane. The high efficiency of squalene to promote the formation of the inverse hexagonal phase is discussed along the lines of argument based on the model of Kirk et al. (Kirk, G.L., Gruner, S.M. and Stein, D.E. (1984) Biochemistry 23, 1093–1102).

Introduction

Research on the interaction of small hydrophobic molecules and phospholipid model membranes has been stimulated by a broad range of interests including aspects like the anesthetic action of short-chain alkanes or simply to serve as a model system for lipid soluble molecules [1]. Most of these studies dealt with the effects of alkanes on the lamellar-gel to the lamellar liquid-crystalline phase transition of phosphatidylcholines (PC). Although a decade ago Hornby and Cullis [2] reported that addition of *n*-alkanes decreases the lamellar liquid-crystalline-to-inverse-hexagonal phase transition temperature of phosphatidylethanolamines (PE), only recently the number of investigations in this field has been increasing, mainly to test the model of Kirk et al. [3]. According to this model it costs free energy to pack the hydrocarbon chains in the non-homogeneous environment of the inverse hexagonal (H_{II}) phase. This hydrocarbon packing stress should be relieved by the addition of hydrophobic molecules, which are able to fill the interstices of the H_{II}-tubes. In fact it was shown that the incorporation of *n*-alkanes stabilizes the H_{II}-phase of PE [4,5] of PE/PC-mixtures [6,7] and of *N*-monomethylated dioleoylphosphatidylethanolamine (DOPE-Me) [8,9]. Furthermore, Sjölund et al. [10,11] found that larger fractions of alkanes induced the formation of H_{II}-phases even in PC membranes, which are considered as bilayer stabilizing lipids [12], and that cyclooctane and 2,3,4-trimethylpentane, two structural isomers of *n*-octane, had the same effect. Another branched hydrophobic molecule, pristane, an isoprenoid C_{19}-isoalkane, was shown to transform at least part of a dioleoyl-PE/PC

* Corresponding author. Fax: +43 316 812367.

Abbreviations: SOPE, 1-stearoyl-2-oleoylphosphatidylethanolamine; POPC, 1-palmitoyl-2-oleoylphosphatidylcholine; DOPE, dioleoylphosphatidylethanolamine; DOPE-Me, *N*-monomethylated dioleoylphosphatidylethanolamine; PC, phosphatidylcholine; PE, phosphatidylethanolamine; DSC, differential scanning calorimetry; SAXD, small-angle X-ray diffraction; L_β, lamellar gel; L_α, lamellar liquid-crystalline; H_{II}, inverse hexagonal; T_{LH}, L_α-H_{II} phase transition temperature; T_m, L_β-L_α phase transition temperature or main transition temperature; $\Delta T_{1/2}$, transition halfwidth; ΔH_{cal}, calorimetric enthalpy; ΔH_{vH}, van't Hoff enthalpy; n, cooperativity; $\Delta C_{p,max}$, maximum excess heat capacity.

mixture (3:1, mol/mol) into an H_{II}-phase and to lower the main transition of this system by 0.6°C [13]. In this study the effects of squalene on PE/PC membranes were investigated, as squalane, the saturated analog, was shown to be very effective in promoting the H_{II}-phase in DOPE-Me membranes [9].

Squalene is an intermediate in the biosynthesis of sterols and as such a common cellular component. Cellular concentrations are usually low, but can vary depending on growth conditions. For example, in facultative anaerobes such as baker's yeast, *Saccharomyces cerevisiae*, cease of sterol synthesis under anerobic conditions leads to a several-fold increase in squalene concentration [14]. This still moderate level of squalene is obviously tolerated by *S. cerevisiae*. However, large quantities of squalene accumulating in fungi treated with specific inhibitors of squalene epoxidase [15] lead to growth inhibition and, with some organisms, to cell death. Inhibitors of squalene epoxidase, the so-called allylamines, are therefore in clinical use as powerful antifungal drugs [16]. The molecular mechanism underlying the fungistatic or fungicidal effect of squalene accumulation is not clear, but the hydrophobic character of squalene suggests that this compound, when present in high concentrations, might disturb membrane structures and interfere with membrane-associated cellular processes [17]. Testing of the hypothesis that squalene was indeed a powerful membrane perturbant was a further incentive to this study.

High-precision differential scanning calorimetry (DSC) as well as small- and wide-angle X-ray diffraction were used to elucidate the phase behavior of stearoyloleoyl-PE (SOPE)/palmitoyloleoyl-PC (POPC) model membranes in the presence of squalene. Our results demonstrate that both the lamellar gel to lamellar liquid-crystalline (L_β-L_α) and lamellar liquid-crystalline to inverse hexagonal (L_α-H_{II}) phase transition are affected by squalene, although to a different extent. The small, but significant decrease of the main transition temperature indicates the destabilization of the gel phase and a preference of squalene for the liquid-crystalline phase. On the other hand, the L_α-H_{II} phase transition is dramatically shifted to lower temperatures and is even overlapping with the L_β-L_α phase transition around 6 mol% squalene corresponding to about 3.9 lipid volume % squalene. This finding will be discussed in terms of the model established by Gruner and co-workers [3,4,18].

Materials and Methods

Lipids. 1-Stearoyl-2-oleoylphosphatidylethanolamine [19] and 1-palmitoyl-2-oleoylphosphatidylcholine [20] were synthesized as described. The phospholipids were found to be better than 98% pure by GLC analysis of fatty acid methyl esters. Thin-layer chromatography showed only one single spot using $CHCl_3$/CH_3OH/H_2O (65:25:4, v/v) or $CHCl_3$/CH_3OH/NH_3 (50:25:6, v/v) as a solvent. Squalene was purchased from Merck, Darmstadt (Germany) and its purity was also checked by GLC.

Liposome preparation. Appropriate amounts of the lipid stock solutions in $CHCl_3$/CH_3OH (2:1, v/v) were mixed to yield the desired lipid mixture, dried under a stream of nitrogen and finally in vacuo over phosphorus pentoxide for about 6 h. Subsequently, the lipids were dispersed in excess deionized water and hydrated for several hours with periodical, extensive vortex mixing around 35°C, which is above the main transition temperature of pure SOPE liposomes [21,22]. With increasing squalene content it became successively more difficult to prepare homogeneous lipid dispersions and hence, additionally, mechanical agitation as well as cycling through the phase transition range was applied. Still, larger lipid aggregates were observed at admixtures of squalene ≥ 5 mol%. All samples were kept then for 1 week at about 4°C before measurements. The exact amount of phospholipid was determined according to the method of Bartlett [23] and squalene content by GLC using stigmasterol as an internal standard. The phospholipid concentration was in the range of 0.5–1 mg/ml for microcalorimetric experiments and about 50 mg/ml for X-ray diffraction measurements. In order to be able to compare the effects of the addition of different hydrophobic molecules it is necessary to calculate the actual hydrophobic volume added to the phospholipids, following a procedure described by Siegel et al. [9]:

$$\text{lipid volume\% additive} = [(W_{add}/\delta_{add})/(W_{Lip}/\delta_{Lip} + W_{add}/\delta_{add})] \times 100$$

where W_{add} is the weight of the additive (in our work squalene) and W_{Lip} the weight of the phospholipid in the sample, respectively; δ_{add} and δ_{Lip} are their respective densities at 20°C. A value of 0.8584 g/ml was taken for squalene from the CRC Handbook of Chemistry and Physics, whereas a density of 1 g/ml was assumed for the SOPE/POPC mixture.

Differential scanning calorimetry (DSC). In order to monitor the lipid polymorphism, a high-sensitivity, adiabatic scanning calorimeter DASM-4 (Biopribor, Pushchino, Russia) designed by Privalov et al. [24] was used at a scan-rate of 0.25 K/min. The cells were pressurized with nitrogen to about 2 atm to prevent bubbling on heating and loss of solvent by evaporation. The calorimeter was calibrated by the internal electrical power signal and was interfaced to an IBM-AT computer by a lab-built 8 bit analog/digital conversion board for automatic data collection. Calorimetric enthalpies (ΔH_{cal}) were calculated by integrating the peak areas after subtracting the instrumental baseline.

X-ray diffraction. X-ray diffraction experiments were performed on a modified Kratky compact camera (SWAX, MBraun-Graz-Optical Systems, Graz, Austria) adapted for simultaneous recording of diffraction data in both the small- and wide-angle region as described in detail by Laggner and Mio [25]. Ni-filtered CuKα-radiation (λ = 1.54 Å) originating from a rotating anode (Rigaku-Denki, Japan) with a power of 2 kW was used. The camera was equipped with a Peltier controlled variable-temperature cuvette and two linear one-dimensional position-sensitive detectors OED 50-M (MBraun, Garching, Germany), which were placed at a sample-to-detector distance of 26.5 cm (small-angle range) and 32 cm (wide-angle range), respectively. Temperature control was achieved by the programmable temperature-control equipment MTC-2.0 (MBraun-Graz-Optical Systems, Graz, Austria). Diffractograms were recorded with exposure times of 1000 s, after the samples were equilibrated at the respective temperature for 15 min. Bragg spacings, deduced from these diffractograms, exhibit an error up to 1 Å.

Results

Thermodynamic parameters calculated from calorimetric experiments for pure SOPE liposomes (thermogram not shown) are summarized in Table I. Phase assignment, performed earlier in our laboratory [22], showed that the low temperature transition is due to a structural change from the lamellar-gel (L_β) phase to the lamellar liquid-crystalline (L_α) phase and the high temperature transition is due to a transition from the L_α-phase to the inverse hexagonal (H_{II}) phase, with corresponding transition temperatures of 30.8°C (30.4°C were reported from light scattering experiments by Stoffel and Michaelis [21]) and 55°C, respectively. On reheating the L_β-L_α phase transition was reversible, but broadened, characterized by an increase of the transition halfwidth ($\Delta T_{1/2}$) by about 20% with a concomitant decrease of the maximum excess heat capacity ($\Delta C_{p,max}$). The enthalpy of the main transition is 5.2 kcal/mol with an experimental error of ±0.4 kcal/mol. An enthalpy of 4.5 kcal/mol was reported for 1-palmitoyl-2-oleoylphosphatidylethanolamine [26], which is in good agreement with the value calculated for SOPE, if one considers that the enthalpy of the main transition contains a chain length independent and dependent term, where the latter was estimated to be 0.52 kcal/mol CH_2 for disaturated phosphatidylethanolamines [27]. The enthalpy of the L_α-H_{II} transition is usually found to be in the order of 5–15% of the main transition enthalpy [28], whereas the value of 1.0 kcal/mol obtained in this study is around 20%. However, it should be mentioned that the data obtained for this transition are in general of poor accuracy because of its broadness and low magnitude.

In order to avoid problems in preparing homogeneous phosphatidylethanolamine dispersions [26,29,30], we studied the effects of squalene on mixtures composed of 95 mol% SOPE and 5 mol% POPC, further called SOPE/POPC. The latter phospholipid undergoes the main transition just below 0°C [31,32]. Addition of such an amount of POPC decreases the L_β-L_α phase transition temperature (T_m) by 1°C and increases the L_α-H_{II} phase transition temperature (T_{LH}) by 9°C. Whereas the width and shape of the high temperature transition remains unaffected by the presence of POPC, the main transition is broadened and the asymmetry of this transition is more pronounced. X-ray diffraction

TABLE I

Calorimetric parameters of the phase transitions of aqueous phospholipid / squalene dispersions

		Phase transition:	L_β-L_α				L_α-H_{II}	
Phospholipid	Mol% squalene	T_m (°C)	$\Delta C_{p,max}$ (kcal/K.mol)	ΔH_{cal} (kcal/mol)	ΔH_{vH} (kcal/mol)	n [a]	T_{LH} (°C)	ΔH_{cal} (kcal/mol)
SOPE	0	30.8	3.0	5.2	398	75	55 (59) [b]	1.0
SOPE+	0	29.8	2.0	5.1	285	56	64 (68) [b]	1.2
5 mol% POPC	1 (0.6) [c]	28.6	1.8	5.2	246	47	61 (65) [b]	1.4
	2 (1.3)	28.6	1.2	5.2	170	33	52	1.6
	5 (3.3)	28.1 (29) [b]	1.4	5.4	n.c. [d]	n.c.	40	1.3
	6 (3.9)	28.8 (~ 26, 28.2) [b]	1.5	5.7	n.c.	n.c.	n.d. [e]	n.d.
	10 (6.6)	28.6 (~ 26, 28.1) [b]	1.6	5.6	n.c.	n.c.	n.d.	n.d.

[a] $n = \Delta H_{vH} / \Delta H_{cal}$, average cooperative unit of phospholipid molecules.
[b] Shoulder at indicated temperature.
[c] Values in parentheses correspond to lipid volume % squalene (for calculation see methods).
[d] n.c., no values calculated owing to overlapping phase transitions.
[e] n.d., no transition discernible.

experiments performed with the SOPE/POPC mixture show the same phase sequence ($L_\beta \rightarrow L_\alpha \rightarrow H_{II}$) as described before for pure SOPE liposomes. Wide-angle X-ray diffraction experiments gave the typical patterns of the various phases [33]. In the L_β-phase a sharp, symmetric peak at 4.2 Å, characteristic for a hexagonal packing of the hydrocarbon chains oriented normal to the bilayer plane, and in both the L_α and H_{II} phase a broad, diffuse peak centered around 4.4 Å, characteristic for hydrocarbon chains in the fluid state, were observed. Increasing the temperature from 2°C to 20°C leads to a slight decrease of the lamellar repeat distance of the L_β-phase from 66 to 64.4 Å. At 28°C, where – according to the DSC curve (Fig. 1A) – the L_β-L_α phase transition is already under progress, the intensity of the first-order reflection of the L_β-phase decreases and a shoulder arises at about 55 Å, indica-

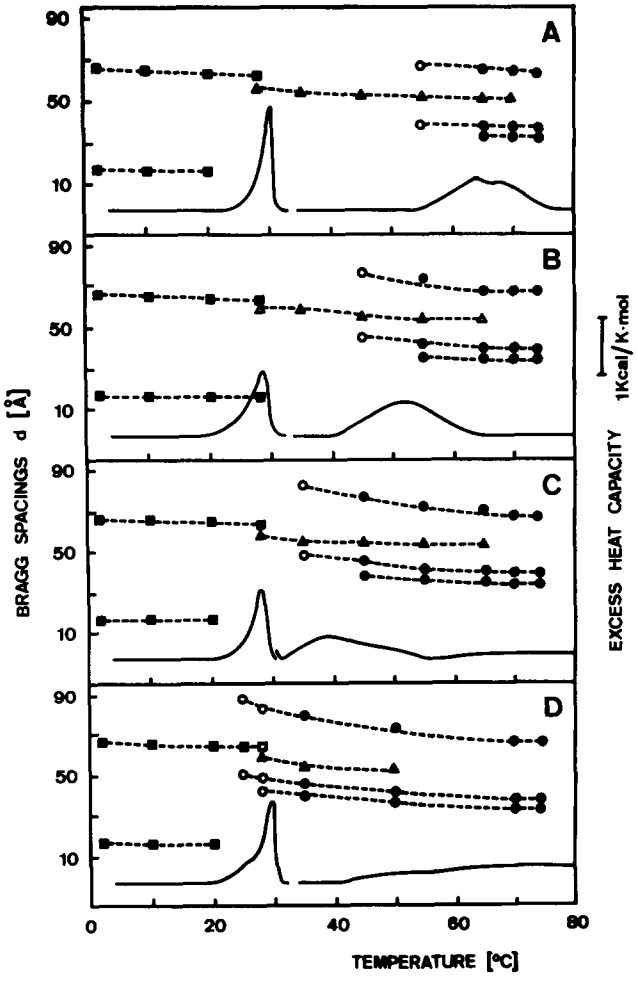

Fig. 1. Normalized excess heat capacity curves (———) and Bragg spacings (— — —) of aqueous dispersions of SOPE/POPC without squalene (A) and in the presence of 2 (B), 5 (C) and 10 (D) mol% squalene, respectively. The part of the thermograms corresponding to the $L_\alpha \rightarrow H_{II}$ transition range was enlarged by a factor of 5 and smoothened by hand. ■ L_β-phase ▲ L_α-phase ● H_{II}-phase. Open symbols indicate minor amounts of the corresponding phase.

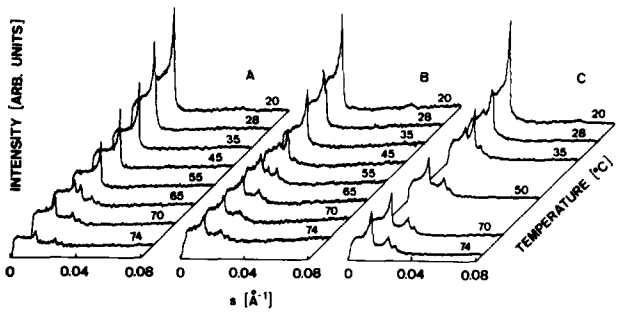

Fig. 2. Small-angle X-ray diffractograms of aqueous dispersions of SOPE /POPC without squalene (A) and in the presence of 5 (B) and 10 (C) mol% squalene, respectively; where $s = 2\sin\Theta/\lambda$ (2Θ = scattering angle, λ = wavelength).

tive for the appearance of the L_α-phase. Diffraction patterns around T_{LH} show a coexistence of the L_α and H_{II} phase with first order reflections of 52.7 Å and 66.5 Å, respectively (Figs. 1A and 2A). Increasing the temperature to 74°C gives rise to a diffraction pattern with Bragg reflections indexing in the ratio of $1:1/\sqrt{3}:1/2:1/\sqrt{7}$, characteristic for hexagonally packed tubes of a pure H_{II} phase [34]. It should be noted here, that also for all samples with squalene the same general behavior concerning the X-ray diffraction patterns was observed. The lamellar repeat distances of the L_β-phase are even identical. Again the first order reflections of both the L_α and H_{II} phases decrease with increasing temperature being slightly, but significantly increased for both phases as compared to the SOPE/POPC mixture (Fig. 1). Such a temperature dependence has already been described earlier for diradyl-PE/POPC mixtures [30] as well as for dioleoyl-PE [35]. In the latter study it was demonstrated that the decrease of the H_{II} lattice is due to the growing disorder of the phospholipid's side-chains, which results in a smaller water core of the H_{II} tube.

The calorimetric enthalpy of the main transition remains practically constant up to an addition of 5 mol% squalene. However, the other transition parameters are significantly affected by the presence of this hydrophobic molecule (Table I, Fig. 1). At 1 mol% squalene T_m is reduced by 1.2°C and $\Delta T_{1/2}$ is slightly increased. The effect on the L_α-H_{II} transition is still relatively small, namely a decrease of T_{LH} by about 3°C and a slight increase of the transition range. Increasing the amount of squalene to 2 mol% does not further change the main transition temperature, but leads to a further broadening of this transition. However, the L_α-H_{II} phase transition is markedly affected, as the temperature is lowered by more than 10°C as compared to the pure phospholipid mixture. Small-angle X-ray diffraction (SAXD) experiments showed that at 28°C, close to the main transition midpoint, the first order reflection is broadened with a shoulder around 60 Å, giving raise to a Bragg spacing of 58.6 Å for the

L_α-phase at 35°C and that above 65°C only a diffraction pattern, which is typical for a pure H_{II} phase, is seen with a first order reflection of about 68 Å at this temperature (Fig. 1B).

In phospholipid mixtures containing 5 mol% squalene T_m is decreased to 28.1°C and a small shoulder is detectable at about 29°C (Table I, Fig. 1C), which might be due to the onset of the L_α-H_{II} phase transition, centered around 40°C. The small-angle X-ray diffractogram at 28°C shows two reflections, one corresponding to the L_β-phase (63.6 Å) and one to the L_α-phase (58.6 Å). The H_{II} phase is characterized by a first order reflection of 69 Å at 65°C.

The phase behavior of SOPE/POPC is dramatically affected in the presence of 6 and 10 mol% squalene, respectively. Within the experimental limits practically identical results were obtained from microcalorimetric and X-ray diffraction experiments for both lipid systems. No L_α-H_{II} phase transition is distinguishable from the calorimetric traces and the main transition is of a complex shape (Fig. 1D). At the first sight it seems that T_m is now increased by about 0.5°C as compared to SOPE/POPC with 5 mol% squalene. However, there is still a shoulder at 28.1°C with a similar excess heat capacity value as observed for T_m in the 5 mol% squalene SOPE/POPC mixture and a second smaller one around 26°C. Although there were difficulties to determine precisely the onset of the transition, owing to the strong tailing of the low temperature side, the increased enthalpy of about 0.5 kcal/mol as compared to the pure phospholipid system can be regarded as significant. A closer inspection of the X-ray diffractograms at 28°C indicates the coexistence of all three phases, L_β, L_α and H_{II}, i.e., the L_α-H_{II} transition is overlapping with the L_β-L_α transition, resulting in the complex thermogram. Small- and wide-angle X-ray diffractograms, as shown for SOPE/POPC with 6 mol% squalene in Figs. 3 and 4, clearly demonstrate the coexistence of the different lipid structures. Both X-ray patterns remain unaffected up to 20°C. At 25°C a small peak at about 88 Å as well as the reduced intensity of the wide-angle peak indicate the onset of the H_{II} phase transformation. At 28°C the $d_{(1,0)}$-reflections of all three phases are observed in the small-angle range, while in the wide-angle range the diffraction peak at 4.2 Å is now superimposed onto a broad diffuse peak around 4.4 Å indicative for the appearance of the fluid phases. A midpoint of the lamellar to inverse hexagonal phase transition around 36°C was estimated from the SAXD data. The lamellar repeat distances for the L_α phase were calculated to be 58.6 Å (28°C) and 54.9 Å (35°C). The first order reflection of the H_{II} phase is decreasing from 85 Å (28°C) to about 68 Å (65°C).

Phase boundaries were derived from the thermograms based on the onset and completion point of the transition (Fig. 5). In general, these points are determined as the intersection of the peak slopes with the baseline of the thermograms [36]. However, owing to the asymmetry and large width of the transitions, we

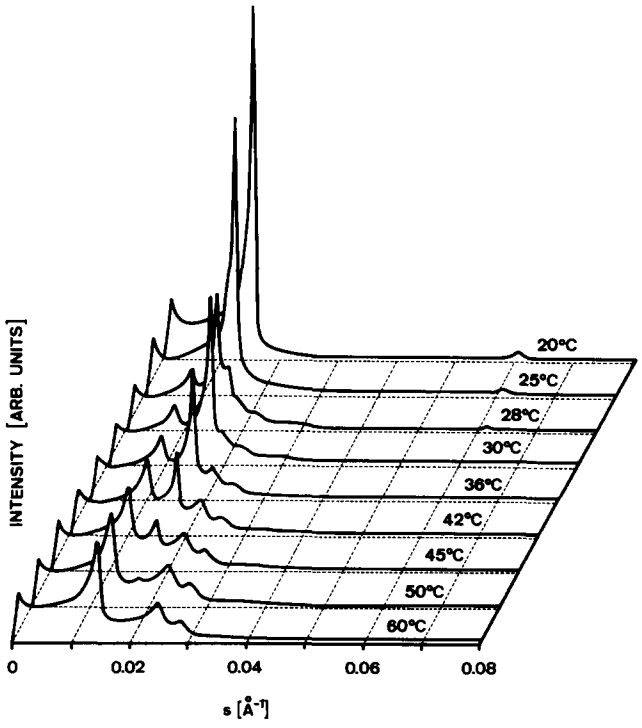

Fig. 3. Temperature dependence of small-angle X-ray diffractograms of aqueous dispersions of SOPE /POPC in the presence of 6 mol% squalene, where $s = 2\sin\Theta/\lambda$ (2Θ = scattering angle, λ = wavelength).

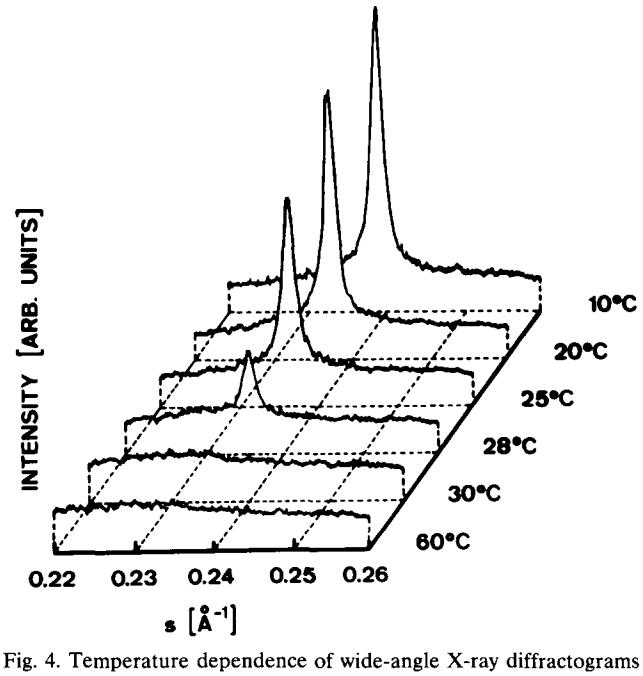

Fig. 4. Temperature dependence of wide-angle X-ray diffractograms of aqueous dispersions of SOPE/POPC in the presence of 6 mol% squalene, where $s = 2\sin\Theta/\lambda$ (2Θ = scattering angle, λ = wavelength).

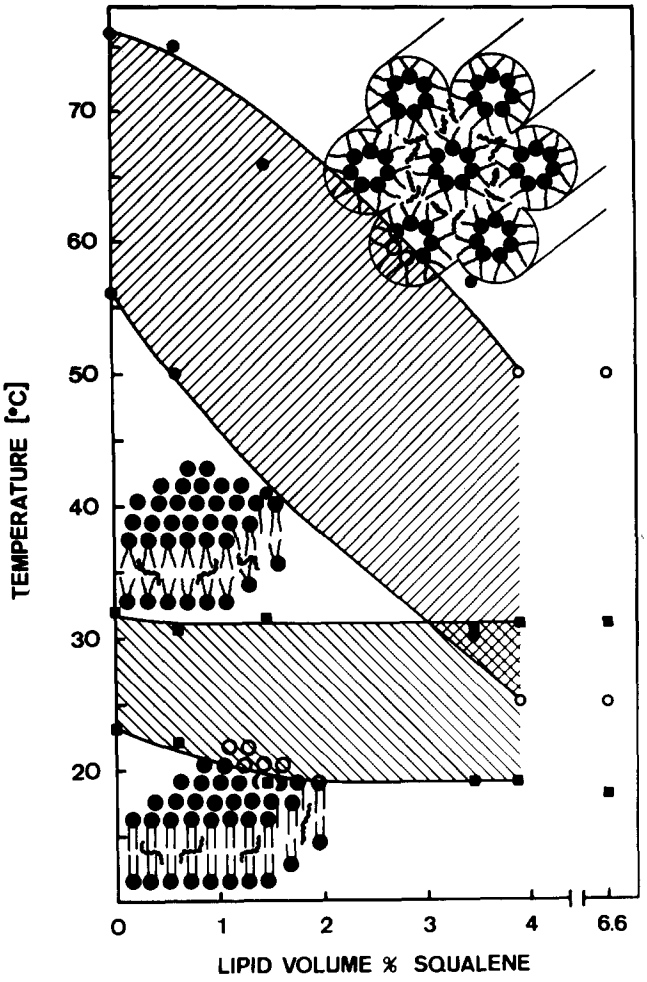

Fig. 5. Phase boundaries of aqueous dispersions of SOPE/POPC in the presence of squalene. Boundaries at 3.9 and 6.6 lipid volume% squalene were estimated from SAXD data. Schemes of the respective phases are indicated in the figure. squalene ~~~ phospholipids .

defined these points, where the transition curves deviate from the linearly extrapolated baselines. The result obtained in this manner is consistent with the X-ray diffractograms. The phase boundaries of the L_α-H_{II} phase transition of the phospholipid mixture in the presence of 6 and 10 mol% squalene, respectively, were estimated from the SAXD data, where at 25°C traces of reflections corresponding to the H_{II} phase are detectable and where at about 50°C the L_α phase vanishes. From this figure it is obvious that above 5 mol% squalene the main transition is overlapping with the transformation of the lamellar phase into the non-bilayer H_{II} phase.

Discussion

The phase behavior of pure SOPE liposomes and of mixtures composed of 95 mol% SOPE and 5 mol% POPC was studied by DSC and X-ray diffraction. Addition of the bilayer stabilizing phospholipid, POPC, which is in the lamellar liquid-crystalline phase in the temperature range of interest, has a small effect on the L_β-L_α phase transition, but a considerable effect on the L_α-H_{II} transition, which was already reported a decade ago for other PE/PC mixtures of similar chain length [for example, Refs. 37–39]. In the phospholipid mixture $\Delta T_{1/2}$ is increased indicating a loss of cooperativity. This decrease of the average cooperative unit of phospholipid molecules can be estimated from the ratio of van't Hoff enthalpy (ΔH_{vH}) to calorimetric enthalpy [for example, Ref. 40], where ΔH_{cal} is equal to the area under the transition curve and ΔH_{vH} can be determined from the calorimetric experiments according to the standard formula:

$$\Delta H_{vH} = 4RT_m^2 \cdot \Delta C_{p,max} / \Delta H_{cal}$$

where $\Delta C_{p,max}$ is the maximum excess heat capacity and R is the gas constant. Incorporation of squalene into SOPE/POPC mixtures decreases both the cooperativity of the transition and to a minor (compared to the depression of T_{LH}) but significant extent T_m, which indicates a slightly higher affinity for the lamellar liquid-crystalline phase. A similar result was also reported for dielaidoyl-PE liposomes in the presence of the C_{20}-saturated alkane, eicosane, and its monounsatured analog, eicosene [5]. But otherwise the effect of hydrophobic molecules on the main transition of PE-liposomes has been rarely studied, although numerous data have been acummulated for disaturated PC/alkane mixtures [1 and refs. therein]. These studies showed that the incorporation of short-chain *n*-alkanes ($C < 12$) into dimyristoylphosphatidylcholine liposomes [41,42] caused the same effects on the L_β-L_α phase transition as observed in our systems. By means of neutron diffraction [41,43] and ^2H NMR spectroscopy (for example, Refs. 44,11,9), it was shown that alkanes are predominantly located in the most disordered region of the bilayer interior, and avoid the entropically less favorable acyl chain region between C_2-C_{10}, which was shown to be more ordered (for example, Ref. 45). The disordered region is, of course, larger the longer the phospholipid's acyl chain and, therefore, longer chain alkanes should be dissolved in such membranes, which was in fact observed for disaturated PC/alkane mixtures of different chain lengths [44]. Additionally, it was reported in the same study that the solubility was still larger in membranes of egg PC, which contains also unsaturated acyl chains. On the contrary, if the alkane chain length exceeds a certain critical length, this optimized packing is disturbed and some molecules will align parallel to the acyl chain of the phospholipid, reaching into the plateau region mentioned above, which results in a higher affinity for the gel phase causing an increase of T_m. In analogy to these observations we can conclude that squalene must be able to

locate in the most disordered region of the bilayer, which might be indicative, that squalene rather adopts a coil than an extended conformation, when it is located in the bilayer interior.

Recently, an increasing number of systematic studies on the L_α-H_{II} phase transition in the presence of alkanes have been reported, mainly to get insight into the driving forces of this transition [cf. 46]. In our study, we found that the addition of 2 mol% squalene is sufficient to compensate the bilayer stabilizing effect of 5 mol% POPC (Table I). Increasing further the amount of squalene depresses dramatically T_{LH} (Fig. 6) and at 6 mol%, i.e., 3.9 lipid volume % squalene both transitions are overlapping to a great extent (Fig. 5). The roughly linear decrease of T_{LH} up to an addition of 3.9 lipid volume% squalene indicates that no separate neat phases are formed within this concentration range, consistent with observations by Siegel et al. [9] for monomethylated dioleoyl-PE in the presence of different alkanes. The H_{II} lattice spacing (a_{HII}), i.e. the diameter of the H_{II} tube, shows also a roughly linear dependence on added squalene within this concentration range (Fig. 6). As this parameter, which can be calculated from the $d_{(1,0)}$-Bragg spacing by $a_{HII} = (2/\times\sqrt{3}) \cdot d_{(1,0)}$, is dependent on temperature, the data are compared at a temperature $T = T_{LH} + 15°C$, which correlates approximately with the appearance of a solely H_{II} phase. On the other hand, a further increase of the squalene concentration does neither change T_{LH} nor the tubular dimension of the H_{II} phase (Fig. 6). This fact can be explained by the circumstance that in our model system the partition of squalene is limited to about 4 lipid volume %. This is supported by observations by Turner and Gruner [47], who assumed from

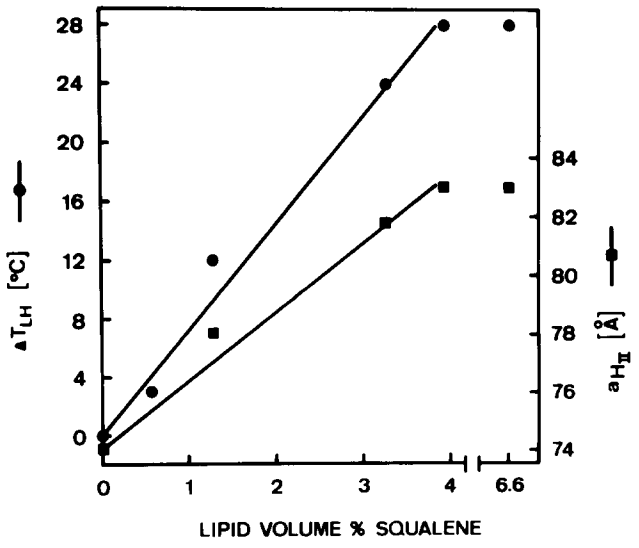

Fig. 6. H_{II} lattice spacing (a_{HII}) and depression of T_{LH} (ΔT_{LH}) in the presence of squalene, where $a_{HII} = (2/\sqrt{3}) \cdot d_{(1,0)}$ and $d_{(1,0)}$ is the first order reflection of the H_{II} phase and $\Delta T_{LH} = T_{LH,SOPE/POPC} - T_{LH,SOPE/POPC+Squalene}$.

TABLE II

Comparison of the efficiency to depress T_{LH} (ΔT_{LH}) by different hydrophobic molecules at constant added volume in model membranes

Phospholipid	Additive	ΔT_{LH}[°C]/ lipid vol%
SOPE+5 mol % POPC	squalene	7
egg PE [a]	dodecane	4
	hexane	4
DOPE-Me [b]	squalane	20
	dodecane	10

[a] Data calculated from results reported by Hornby and Cullis [2].
[b] Data taken from Siegel et al. [9].

their estimations of the actual volume of squalene incorporated into the H_{II} phase of dioleoyl-PE (DOPE) that just half of the squalene, added to their preparation (initial concentration was 10% (w/w)), was incorporated, which would suggest a partition limit in the range of 5 lipid volume %. Although this calculation is only a crude one, the higher partition could be understood considering that the solubility of alkanes increases with increasing degree of unsaturation as was demonstrated for PC membranes [44].

It is of interest to compare the effectiveness of added squalene to depress T_{LH} with other hydrophobic molecules (Table II). From Fig. 6 we can calculate that squalene decreases the lamellar to inverse hexagonal phase transition by about 7°C/lipid volume %. From data reported for egg PE in the presence of different *n*-alkanes [2] we calculated a decrease of T_{LH} by ~ 4°C/lipid volume %. This means that squalene is about twice as efficient as *n*-alkanes, although we are aware of the differences in both model systems. However, this result compares well with the observations in DOPE-Me systems, where the saturated analog of squalene, squalane, was also twice effective as compared to *n*-alkanes [9]. But note that the efficiency of the hydrophobic molecules in the latter system is again increased by a factor of 2 to 3 as compared to the PE system, which can be attributed to the differences in the phospholipid headgroup. It was demonstrated already before that the incorporation of small amounts of hydrophobic molecules lower drastically T_{LH} [2,4,9], which can be explained along the lines of argument established by Gruner and coworkers [3,4,48]. These authors proposed that the constraints of hydrocarbon chain packing, owing to the anisotropic packing requirements in the H_{II} tube, are reduced by filling the interstitial spaces between the hexagonally packed phospholipid tubes with the hydrophobic molecules. As outlined before, squalene will tend to dissolve in the most disordered region of the hydrophobic core, which enables these molecules to fill the perimeters and corner regions of the hexagons. Results reported recently by Siegel et al. [9], Turner and Gruner [47] and

Turner et al. [49] support this model. Siegel et al. [9] showed by ^2H NMR using deuterated squalane, that this hydrophobic molecule is in fact in a more disordered environment than the other *n*-alkanes (C_{12-16}) investigated. The same conclusion was obtained from X-ray experiments by Turner and Gruner [47], applying a low-resolution Fourier reconstruction method for the systems DOPE and different amounts of dodecane as well as of DOPE and 10% (w/w) squalene. They found that the anisotropy of the electron density near the methyl-ends of the hydrocarbon chains is reduced in the presence of the hydrophobic molecules. Such a more uniform packing environment for the phospholipid was also found by neutron diffraction experiments with DOPE and deuterated decane [49]. Furthermore in the earlier study, it was shown that in the presence of dodecane or squalene the water core was even relaxed to a circular shape at tubular dimensions > 75 Å, whereas in the pure DOPE system noncircularities were observed caused by the still existing anisotropic packing requirements. However, while the radius of the water core was increased in the presence of squalene, it was reduced with dodecane. It was assumed that the enlarged water core in the DOPE/squalene mixture might be due to relaxation close to the spontaneous radius of curvature of the lipid system probably due to an additional reduction of the azimuthal anisotropic lipid chain packing by the bulky, branched hydrophobic molecule. Our data support this assumption and suggest that SOPE/POPC is able to adopt the preferred radius of spontaneous curvature, when 4 lipid volume % squalene are added.

Results presented in this study demonstrate that squalene in concentrations that can be observed in fungal cells treated with squalene epoxidase inhibitors effectively destabilize the bilayer structure of artificial phospholipid membranes. Although it needs to be established whether or not similar effects can indeed be observed in biological membranes, the results obtained with model membranes support the hypothesis that exceedingly high cellular concentrations of squalene might be detrimental to cellular membranes and eventually cause cell death.

Acknowledgements

Support for this work was provided by the Sandoz Forschungsinstitut, Vienna (Austria) to E. Gnamusch. The authors gratefully acknowledge the expert assistance by Mrs. Annemarie Schmidt in the preparation of this manuscript, especially the artwork.

References

1 Lohner, K. (1991) Chem. Phys. Lipids 57, 341–362.
2 Hornby, A.P. and Cullis, P.R. (1981) Biochim. Biophys. Acta 647, 285–292.
3 Kirk, G.L., Gruner, S.M. and Stein, D.E. (1984) Biochemistry 23, 1093–1102.
4 Kirk, G.L. and Gruner, S.M. (1985) J. Phys. (Les Ulis, Fr.) 46, 761–769.
5 Epand, R.M. (1985) Biochemistry 24, 7092–7095.
6 Tate, M.W. and Gruner, S.M. (1987) Biochemistry 26, 231–236.
7 Rand, R.P., Fuller, N.L., Gruner, S.M. and Parsegian, V.A. (1990) Biochemistry 29, 76–87.
8 Gruner, S.M., Tate, M.W., Kirk, G.L., So, P.T.C., Turner, D.C., Keane, D.T., Tillcock, C.P.S. and Cullis, P.R. (1988) Biochemistry 27, 2853–2866.
9 Siegel, D.P., Banschbach, J. and Yeagle, P.L. (1989) Biochemistry 28, 5010–5019.
10 Sjölund, M., Lindblom, G., Rilfors, L. and Arvidson, G. (1987) Biophys. J. 52, 145–153.
11 Sjölund, M., Rilfors, L. and Lindblom, G. (1989) Biochemistry 28, 1313–1329.
12 Cullis, P.R. and De Kruijff, B. (1979) Biochim. Biophys. Acta 599, 399–420.
13 Gawrisch, K. and Janz, S. (1991) Biochim. Biophys. Acta 1070, 409–418.
14 Fryberg, M., Oehlschlager, A.C. and Unrau, A.M. (1973) J. Am. Chem. Soc. 95(17), 5747–5757.
15 Paltauf, F., Daum, G., Zuder, G., Högenauer, G., Schulz, G. and Seidl, G. (1982) Biochim. Biophys. Acta 712, 268–273.
16 Ryder, N.S. (1992) Br. J. Dermatol. 126, Suppl. 39, 2–7.
17 Gnamusch, E., Ryder, N.S. and Paltauf, F. (1992) J. Dermatol. Treatment 3, 9–13.
18 Gruner, S.M. (1985) Proc. Natl. Acad. Sci. USA 82, 3665–3669.
19 Hermetter, A., Stütz, H., Lohner, K. and Paltauf, F. (1987) Chem. Phys. Lipids 43, 69–77.
20 Hermetter, A., Stütz, H., Franzmeier, R. and Paltauf, F. (1989) Chem. Phys. Lipids 50, 57–62.
21 Stoffel, W. and Michaelis, G. (1976) Hoppe Seyler's Z. Physiol. Chem. 357, 21–33.
22 Laggner, P., Kriechbaum, M., Hermetter, A., Paltauf, F., Hendrix, J. and Rapp, G. (1989) Progr. Colloid Polym. Sci. 79, 33–37.
23 Bartlett, G.R. (1959) J. Biol. Chem. 234, 466–468.
24 Privalov, P.L., Plotnikov, V.V. and Filimonov, V.V. (1975) J. Chem. Thermodyn., 41–48.
25 Laggner, P. and Mio, H. (1992) Nucl. Inst. Meth. Phys. Res. A 323, 86–90.
26 Epand, R.M. and Bottega, R. (1988) Biochim. Biophys. Acta 944, 144–154.
27 Marsh, D. (1990) in CRC Handbook of Lipid Bilayers (Marsh, D., ed.), pp. 135–137, CRC Press, Boca Raton.
28 Seddon, J.M. (1990) Biochim. Biophys. Acta 1031, 1–69.
29 Malthaner, M., Hermetter, A., Paltauf, F. and Seelig, J. (1987) Biochim. Biophys. Acta 900, 191–197.
30 Lohner, K., Balgavy, P., Hermetter, A., Paltauf, F. and Laggner, P. (1991) Biochim. Biophys. Acta 1061, 132–140.
31 De Kruijff, B., Demel, R.A., Slotboom, A.J., Van Deenen, L.L.M. and Rosenthal, A.F. (1973) Biochim. Biophys. Acta 307, 1–19.
32 Davies, P.J., Fleming, B.D., Coolbear, K.P. and Keough, K.M.W. (1981) Biochemistry 20, 3633–3636.
33 Tardieu, A., Luzzati, V. and Reman, F.C. (1973) J. Mol. Biol. 75, 711–733.
34 Luzatti, V. (1986) in Biological Membranes (Chapman, D., ed.), Vol. 1, pp. 71–123, Academic Press, New York.
35 Tate, M.W. and Gruner, S.M. (1989) Biochemistry 28, 4245–4253.
36 Mabrey, S. and Sturtevant, J. (1976) Proc. Natl. Acad. Sci. USA 73, 3862–3866.
37 Cullis, P.R. and De Kruijff, B. (1978) Biochim. Biophys. Acta 513, 31–42.
38 Hui, S.W., Stewart, T.P., Yeagle, P.L. and Albert, A.D. (1981) Arch. Biochem. Biophys.207, 227–240.

39 Boni, L.T. and Hui, S.W. (1983) Biochim. Biophys. Acta 731, 177–185.
40 Sturtevant, J.M. (1987) Annu. Rev. Phys. Chem. 38, 463–488.
41 McIntosh, T.J., Simon, S.A. and MacDonald, R.C. (1980) Biochim. Biophys. Acta 597, 445–446.
42 Pope, J.M. and Dubro, D.W. (1986) Biochim. Biophys. Acta 858, 243–253.
43 White, S.H., King, G.I. and Cain, J.E. (1981) Nature 290, 161–163.
44 Pope, J.M., Littlemore, L.A. and Westerman, P.W. (1989) Biochim. Biophys. Acta 980, 69–76.
45 Davies, J.H. (1983) Biochim. Biophys. Acta 737, 117–171.
46 Tate, M.W., Eikenberry, E.F., Turner, D.C., Shyamsunder, E. and Gruner, S.M. (1991) Chem. Phys. Lipids 57, 147–164.
47 Turner, D.C. and Gruner, S.M. (1992) Biochemistry 31, 1340–1355.
48 Gruner, S.M., Cullis, P.R., Hope, M.J. and Tilcock, C.P.S. (1985) Annu. Rev. Biophys. Biophys. Chem. 14, 211–238.
49 Turner, D.C., Gruner, S.M. and Huang, J.S. (1992) Biochemistry 31, 1356–1363.